Nonlinear Modeling of SiGe HBT's up to 50 GHz

Clemens N. Rheinfelder, Frank J. Beißwanger, and Wolfgang Heinrich

***Abstract*— A new large-signal model for SiGe heterostructure bipolar transistors (HBT's) is presented that includes nonideal leakage currents, Kirk-effect, and thermal behavior. The parameters are extracted from S-parameter measurements using a special procedure which is insensitive to tolerances in measurement data. The model yields excellent accuracy for dc and S parameters up to 50 GHz. It proved its usefulness in MMIC oscillator design at 26 and 38 GHz.**

***Index Terms*— Heterojunction bipolar transistors, microwave bipolar transistors, nonlinear circuits, nonlinear modeling, silicon germanium.**

I. Introduction

RECENT developments in the area of Si–SiGe–Si heterostructure bipolar transistors (HBT's) pushed the transit frequencies beyond the 100-GHz limit. $F_{\max}$ and f_t values of 160 and 116 GHz, respectively, were achieved [1], [2]. This qualifies the HBT as a key component in the development of microwave Si-based MMIC's. The most critical issue in MMIC design is the accurate modeling of the active devices. This is true particularly for highly nonlinear circuits such as oscillators.

Compared with the MESFET, large-signal HBT modeling is still in its infancy. Due to the more complicated equivalent-circuit topology, determination of the elements from measurements requires highly sophisticated extraction procedures. On the other hand, the common bipolar large-signal descriptions hold only for lower frequencies and need to be extended to cover the microwave frequency range. Also, SiGe special effects have to be included. Most HBT models available so far [3]–[5], for instance, do not consider the Kirk effect. For an accurate modeling of a double-heterojunction HBT (e.g., the SiGe HBT), however, this phenomenon has to be taken into account, because the additional heterojunction at the base-collector interface causes a pronounced Kirk-effect behavior.

In this paper, a novel model is presented. Its special features are:

- full implementation of the Kirk effect;
- temperature-dependent dc characteristics;
- nonideal leakage currents (saturation);
- reliable extraction of extrinsic elements based on a field-theoretical approach.

The paper is organized as follows. First, the extraction of the small-signal elements is described (Section II). Then, the large-signal dc and RF model is treated in Sections III and IV, respectively. Finally, Sections V and VI provide validation by measurement and the conclusions.

The experimental data refer to a Si–SiGe–Si HBT fabricated by Daimler–Benz, which is used within the SiGe MMIC process.

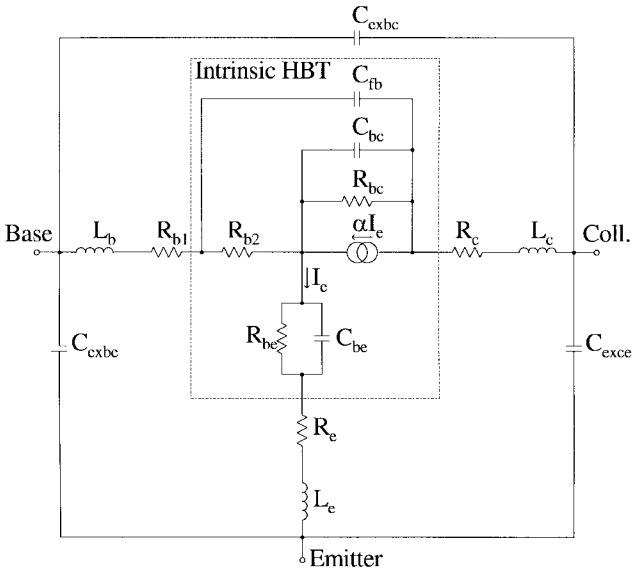

Fig. 1. Small-signal equivalent circuit of the Si–SiGe–Si HBT in the normal active regime. All parasitic extrinsic and intrinsic elements are included.

II. Small-Signal Parameter Extraction

The small-signal equivalent circuit is shown in Fig. 1. The topology results from the physical structure of the SiGe HBT. It is based on the usual T-model with distributed base network to incorporate current crowding, which is unavoidable for the SiGe HBT's under consideration. The current-controlled current source is described by the base-transport factor $\alpha = \alpha_0 e^{-j\omega\tau_\alpha}/(1 + j\omega/\omega_\alpha)$ where α_0 denotes dc current gain in common-base configuration, τ_α is the base transit time, and f_α the 3-dB cut-off frequency $\omega_\alpha/2\pi$. This topology is consistent with the large-signal approach (see Fig. 5). The extrinsic elements, the junction capacitances, and the ratio between the inner and outer base–collector capacitance are directly compatible with the large-signal model, while the bias-dependent intrinsic values are converted according to the large-signal conditions.

Manuscript received March 31, 1997; revised August 15, 1997. This work was supported by the German Bundesministerium für Forschung, Bildung, Wissenschaft und Technologie (BMBF) under Contract 01 M2938 B. The work of F. Beisswanger is supported by the State of Baden-Württemberg within the program for the promotion of young generation scientists.

C. N. Rheinfelder and W. Heinrich are with the Ferdinand–Braun-Institut für Höchstfrequenztechnik, 12489 Berlin, Germany.

F. J. Beißwanger is with Daimler–Benz AG, Forschungszentrum Ulm, 89081 Ulm, Germany.

Publisher Item Identifier S 0018-9480(97)08358-0.

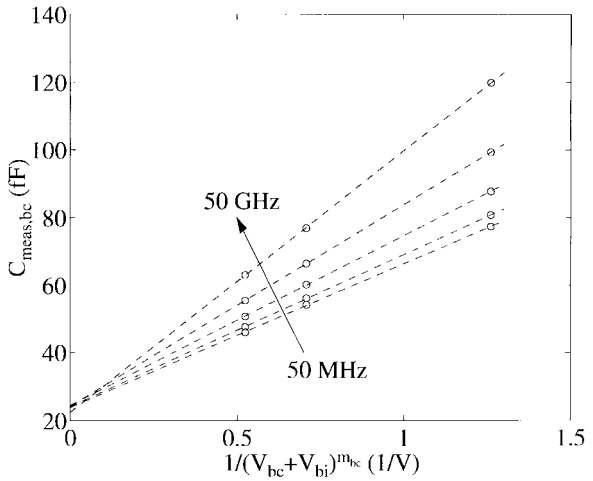

Fig. 2. Extrapolation of base–collector capacitance $C_{\mathrm{meas,\,bc}}$ measured for different frequencies from 0.05 to 50 GHz in cut-off mode. The exponential factor m_{bc} of the junction capacitance is calculated from large-signal measurements of the *C–V* characteristic and the built-in voltage V_{bi} with consideration of bandgap narrowing. The actual value for the base–collector junction is determined to be $m_{\mathrm{bc}} = 0.441$.

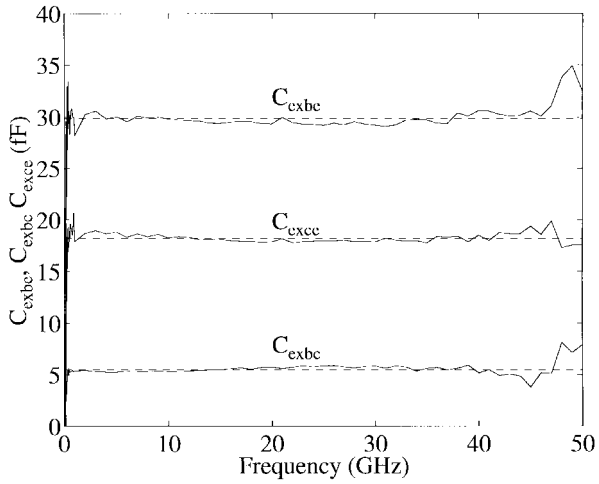

Fig. 3. Extracted pad capacitances for C_{exbc}, C_{exbe}, and C_{exce} in the frequency range between 50 MHz and 50 GHz.

TABLE I
SUMMARY OF EXTRACTED EXTRINSIC ELEMENT VALUES OF A SiGe HBT WITH SIX 1 × 10 μM EMITTER FINGERS

Cap.	[fF]	Ind.	[pH]	Res.	[Ω]
C_{exbe}	30.08	L_b	23.89	R_b	0.94
C_{exbc}	5.23	L_e	3.41	R_e	2.81
C_{exce}	17.79	L_c	21.44	R_c	2.75

The first step in determining the equivalent circuit elements is the accurate extraction of the extrinsic element values. Some of the pad capacitances, pad inductances, and contact resistances are relatively small but have significant influence on the extraction of the intrinsic elements. Thus, their values have to be determined with great accuracy. When applying purely analytical procedures, for instance, extrinsic capacitance and inductance deviations below 1 fF and 1 pH have to be taken into account. Hence, in order to improve accuracy and to establish a realistic parameter range, the contributions of the HBT periphery were investigated by a field-oriented approach (finite difference, frequency domain). The results obtained then serve as a starting point for the following extraction procedure. By determining the parasitic elements by test structures, a significant deviation from the real values occur due to calibration errors and probing offsets. Additionally, the limited accuracy (1%–2%) of the measurement equipment has to be taken into account.

Applying negative bias voltages to the base–emitter and base–collector diodes, the circuit approximately simplifies to the extrinsic and space-charge capacitances and inductances ("cut-off" case) [6]. The extrapolation of these values against infinite negative bias converges to the external capacitance plus an internal part. From the measurement data, these two parts cannot be separated. In the cut-off limit, however, the diode region is fully depleted. Hence, the internal capacitance can be calculated by its parallel-plate approximation $C_{\mathrm{int,\,SCR}} = \varepsilon A_{\mathrm{dio}}/d_{\mathrm{dio}}$, where ε denotes the permittivity of the Si and SiGe region, A_{dio} represents the area of the diode, and d_{dio} is the thickness of the base–emitter and base–collector region, respectively. The measured capacitance value $C_{\mathrm{meas,\,bc}}$ equals the sum of the external part C_{exbc} plus the internal base–collector capacitance $C_{\mathrm{int,\,SCR}}$. Fig. 2 shows the measured base–collector capacitance values $C_{\mathrm{meas,\,bc}}$ and the extrapolation for the cut-off case. For the six-finger HBT under investigation, the above formula yields an inner base–collector capacitance $C_{\mathrm{int,\,SCR}}$ of 18.72 fF. One finds an extrapolated value $C_{\mathrm{meas,\,bc}}$ for $(V_{\mathrm{bc}}+V_{\mathrm{bi}}) \rightarrow \infty$ of 23.95 fF. This results in an extrinsic capacitance $C_{\mathrm{exbc}} = C_{\mathrm{meas,\,bc}} - C_{\mathrm{int,\,SCR}}$ of 5.23 fF. Note that the measured values $C_{\mathrm{meas,\,bc}}$ for different frequencies approach a frequency-independent limit in the cut-off case, as has to be postulated on physical reasons.

In Fig. 3, the extracted values for all extrinsic pad-capacitances in cut-off mode are plotted against frequency in the 50 MHz to 50 GHz range. A remarkably flat frequency response can be observed. This is due to the accurate extraction of all extrinsic elements and reflects the physical situation.

In analogy, by biasing both diodes in the saturation mode ("open-collector") [7], [8], it is possible to determine the extrinsic inductances and the static part of the resistances. Fig. 4 shows the extracted values together with least-square lines for base currents between 12 and 20 mA. With increasing base current, the inductance approaches a constant value over the entire frequency range. This is caused by high carrier injection, which reduces the space-charge region. The characteristics of the inductance L_{b} in Fig. 4 at high base currents clearly supports this explanation. The remaining inductances L_{c} and L_{e} are obtained in a similar way.

In Table I, all static extrinsic elements are summarized. In order to achieve good agreement between measured and simulated curves (Fig. 8), the deviations of these values must remain below a few percent. Especially C_{exbc} and L_{e} show significant influence on the extracted intrinsic elements. Errors at this point cannot be corrected afterwards and lead to nonphysical intrinsic elements. This substantiates the necessity to have reference values for extrinsic elements, which can be obtained only by a 3-D field-oriented approach.

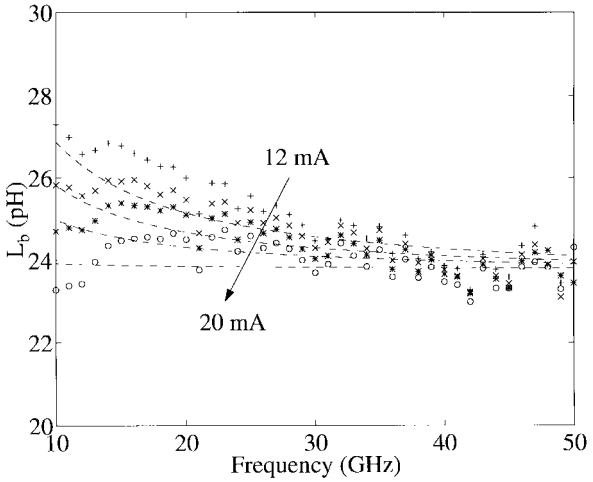

Fig. 4. Variation of base-inductance $L_{\rm b}$ with frequency for base currents between 12 and 20 mA. With increasing base current, the extracted values ($+$, $\times$, *, $\circ$) converge nearly frequency independent to the limit of 23.89 pH (Table I). Additionally, curves in the least-square sense are plotted ($-$).

For the determination of the intrinsic elements, a combination of analytical and statistical methods is applied to suppress the high sensitivity of the small element values to measurement errors and calibration tolerances. The algorithm is based on [9] with significant enhancements regarding stability and wideband extraction. It starts from the measured S parameters from 50 MHz to 50 GHz and solves all equations in a robust least-square sense. The fundamental idea is to subdivide the extraction procedure in several smaller tasks. For example, the base-transport factor α is expressed by the term $|\alpha| = |1-(Y_{11}+Y_{12})/(Y_{11}+Y_{21})|$. Rearranging this expression in a linear least-square sense one obtains α_0, τ_α, and f_α over the entire frequency range. The Y parameters of the intrinsic HBT are determined from Fig. 1 in the usual way. Because no optimization is employed the procedure yields unique results. However, one has to account for ill-conditioning of the least-square matrices. This is accomplished by reordering and scaling of the matrices. Simultaneously, the least-square matrices have to be solved by a QR-algorithm instead of direct matrix inversion to avoid potential errors in the least-square solution.

Table II provides the values of the intrinsic small-signal elements for two different bias points. All values exhibit a behavior as expected from physics. One should point out the strong dependence of the inner base resistance $R_{\rm b2}$ on bias conditions. Also, the base–collector capacitances $C_{\rm bc}$ and $C_{\rm fb}$ change their values significantly. This justifies the distributed description of the base. All extrinsic and intrinsic elements show values that are almost frequency independent up to 50 GHz. This proves the validity of the proposed equivalent circuit (Fig. 1) and of the extraction procedure.

TABLE II
EXTRACTED SMALL-SIGNAL ELEMENT VALUES OF THE SI/SIGE/SI-HBT AT 2 OPERATING POINTS

	OP 1		OP 2	
V_{be}	0.875	V	0.854	V
I_b	0.449	mA	0.599	mA
V_{ce}	2.502	V	4.002	V
I_c	24.31	mA	27.70	mA
R_{be}	1.510	Ω	1.1297	Ω
C_{be}	1.426	pF	2.0763	pF
R_{b2}	10.0761	Ω	7.0977	Ω
R_{bc}	58.105	kΩ	17.435	kΩ
C_{bc}	23.250	fF	17.701	fF
C_{fb}	24.838	fF	21.947	fF
α_0	0.98818		0.98083	
f_α	70.876	GHz	61.868	GHz
τ_α	0.68535	ps	0.68074	ps

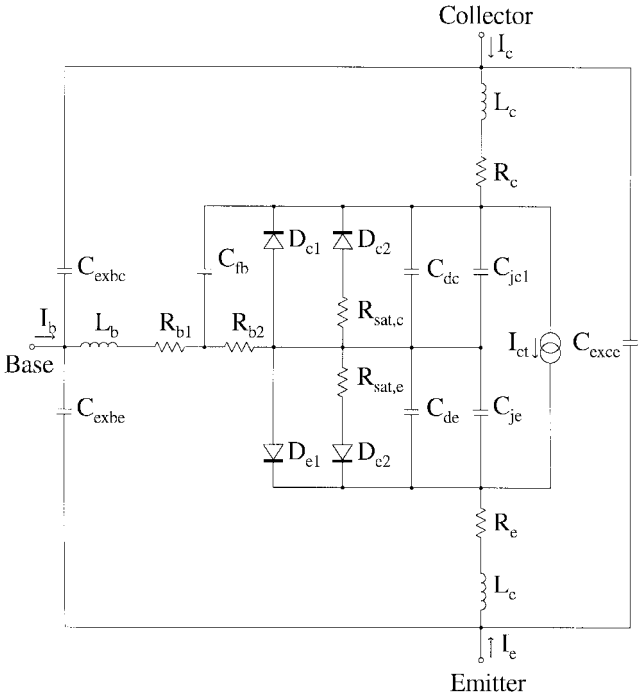

Fig. 5. Extended extrinsic and intrinsic GP model for the SiGe HBT.

III. DC MODELING AND TECHNOLOGY

The nonlinear model (see Fig. 5) is based on the well-known Gummel–Poon (GP) integral base–charge bipolar model [10]. Enhancements regarding the temperature behavior are implemented for the temperature-sensitive parameter values (e.g., $V_{\rm th}$, β, I_s). The increase in temperature is described by a thermal equivalent circuit [5]. Optimum operating conditions for HBT's are at high current densities ($J_C > 10^5$ A/cm^2) [11]. This requires taking the Kirk effect into account. In the standard bipolar-junction transistor (BJT) model, only high injection is considered. Because of the extremely high base doping ($N_A > 10^{20}$ cm^{-3}), this effect can hardly occur in SiGe HBT's but, on the other hand, the Kirk effect gains more influence. At high current densities and low base–collector voltages, the electrons cannot drift fast enough over the base–collector space-charge region and, therefore, partially neutralize the ionized donors in this region. As a result, the neutral base width of the device is increased, which leads to an increased transit time τ_f. This causes the unwanted base pushout and a drop-off in current gain. We include this effect by modifying the integral over the base charge. Because in a

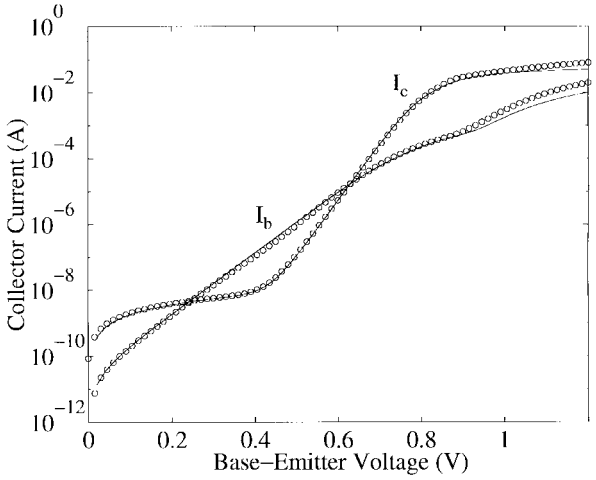

Fig. 6. Measured (∘) and modeled (−) Gummel plot of the SiGe HBT.

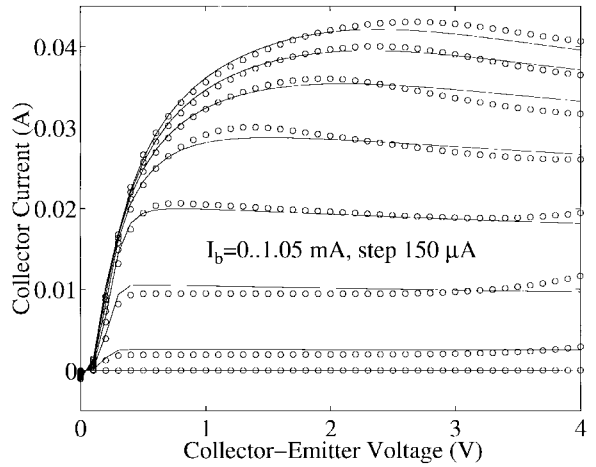

Fig. 7. Measured (∘) and modeled (−) *I–V* characteristics of the SiGe HBT.

HBT the Kirk effect starts more abruptly than in the BJT, the well-known equations [10], [12] need to be modified.

The HBT type under investigation relies on the double-heterojunction SiGe base approach with inversion of the doping levels ($N_{\text{base}} > N_{\text{emitter}}$). Due to the high base-doping level, the base sheet resistance is as low as 550 $\Omega/\square$. Transistors with six 1 μm $\times$ 10 μm emitter fingers reach $f_{\max}$ values of about 85 GHz (MAG).

Figs. 6 and 7 present simulated and measured data for output characteristics and Gummel plot.

In comparison with the standard BJT, one observes significant deviations in the high collector–current regime as well as in the low base–current region. Due to the low-temperature passivation process in conjunction with the double mesa surface, relatively high leakage currents occur, which are dominated by current flow over the surface. Fig. 5 shows the complete large-signal model. In addition to the GP model, two resistors $R_{\text{sat, c}}$ and $R_{\text{sat, e}}$ are included to model the saturation of the leakage currents. Without these resistors, satisfying agreement of the dc curves cannot be achieved. Therefore, the diodes D_{c2} and D_{e2} together with the resistors $R_{\text{sat, c}}$ and $R_{\text{sat, e}}$ describe the nonideal behavior of the space-charge region and surface recombination current.

TABLE III
EXTRACTED LARGE-SIGNAL PARAMETERS FOR THE SI–SIGE–SI HBT

Param.	Value		Param.	Value	
I_s	$2.6{\cdot}10^{-16}$	A	$R_{sat,e}$	260	Ω
I_{se}	$2.5{\cdot}10^{-11}$	A	$R_{sat,c}$	552	Ω
I_{sc}	$1.5{\cdot}10^{-12}$	A	I_{rb}	$1{\cdot}10^{-3}$	A
N_f	1.01		R_{bm}	8.32	Ω
N_r	1.0		R_{bx}	17.67	Ω
N_e	1.86		C_{je}	125.27	fF
N_c	1.32		C_{jc}	88.98	fF
B_f	88		m_{je}	0.359	
B_r	1.2		m_{jc}	0.441	
V_{af}	90	V	V_{je}	0.7713	V
V_{ar}	45	V	V_{jc}	0.7118	V
I_{kf}	0.1	A	X_{cjc}	0.34	
I_{kr}	0.15	A	τ_f	2.45	ps
			τ_r	4.22	ps

All parameter definitions are according to the GP model.

The dc parameters are extracted from the Gummel plot in forward (Fig. 6) and reverse mode. Table III lists all dc and RF parameters of the investigated SiGe HBT.

While the built-in voltages V_{je} and V_{jc} are calculated under consideration of doping and bandgap narrowing [13], the exponential factors m_{je} and m_{jc} are determined by the slope of the intrinsic capacitances in cut-off mode. Caused by the doped spacer between base–collector and base–emitter, the Early voltages V_{af}, V_{ar} are present. These layers are necessary to prevent the outdiffusion of the boron into the collector and emitter. For maximization of the Early voltage, the implementation of an undoped layer is optimal, but this favors the unwanted Kirk effect. The extracted parameters I_{kf} and I_{kr} show that the Webster effect is not significant.

IV. LARGE-SIGNAL MICROWAVE MODELING

The values of the high-frequency-relevant elements were found using small-signal extraction by analytical and statistical methods. Multibias measurements at 100 bias points were performed. The extracted values could be directly implemented in the large-signal model. Fig. 8 shows the measured and simulated S parameters for a typical operating point ($I_{\text{b}} = 450$ A, $I_{\text{c}} = 26$ mA). Excellent agreement is found. The results prove the validity of the new model up to frequencies beyond 50 GHz.

A separate method to validate a large-signal model is to compare simulated and measured output harmonics with the device biased in a typical operating point ($I_{\text{b}} = 450$ μA, $U_{\text{ce}} = 2.5$ V). Fig. 9 presents the corresponding data. The model accurately predicts the fundamental and the first three harmonics. This is an important step in verifying the proposed model, because the input power is swept from small-signal levels up to levels sufficiently large to produce significant gain compression. Therefore, the nonlinearities of the HBT have to be described precisely. At very low input power levels below −20 dBm, the content of the higher harmonics cannot be measured exactly due to the dynamic limitation of the spectrum analyzer. In an amplifier configuration with 50-Ω terminations, the effects of the device's nonlinearities are

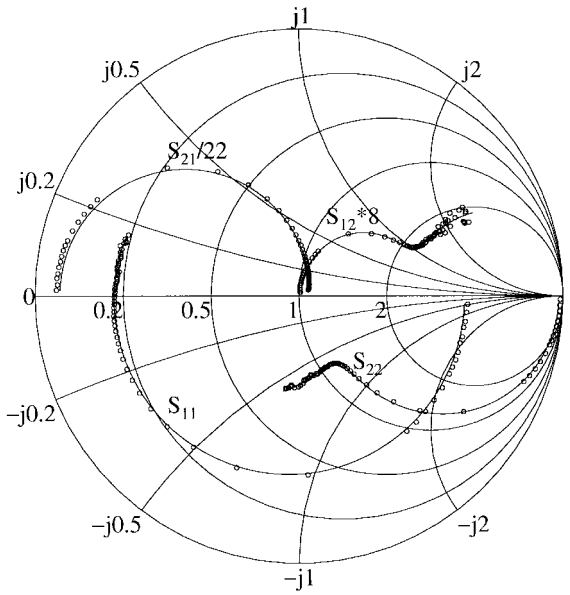

Fig. 8. Measured (∘) and modeled (−) S parameters (f = 0.05–50 GHz) of the SiGe HBT for a typical operating point (I_b = 450 μA, I_c = 26 mA).

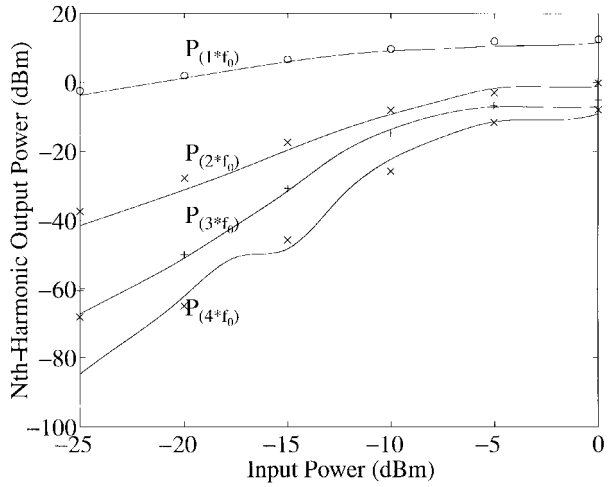

Fig. 9. Comparison between measured (∘, ×, +, ∘) and simulated (−) fundamental and harmonics for the six-finger HBT for one-tone exitation as a function of the available input power. The operating point is I_b = 450 μA, U_{ce} = 2.5 V. The applied fundamental frequency is f_0 = 5 GHz.

minimal. This can be seen in Fig. 9 where the second, third, and fourth harmonic are at least 20 dB below the fundamental level.

A second feature of a new model is compatibility with common circuit-design software. The new model demonstrated numerical stability in harmonic balance and transient analyses for the simulation of oscillators [14] at 38 GHz and amplifiers at 25 GHz.

V. Results

Using the new model in conjunction with large-signal simulations, we designed a monolithically integrated LC oscillator [14]. For fabrication, the Daimler–Benz SiGe process was used. The nominal value for the oscillating frequency was 38.25 GHz. Five oscillators on the same wafer were measured. The maximum output power was 2 dBm. Apart from the fact that the output power is not yet satisfactory, excellent agreement regarding frequency is found. Maximum relative deviation from the nominal frequency is 1.1% (37.818–38.680 GHz). Sixty percent of the measured oscillators show a deviation from the nominal frequency below 0.1%. This proves usefulness and accuracy of our model.

VI. Conclusion

The results demonstrate that the standard nonlinear BJT model can be modified to describe also the microwave HBT case. For SiGe HBT's, nonideal diodes, Kirk effect, and temperature dependence need to be accounted for. A special procedure is applied to extract the small-signal equivalent-circuit parameters. The new model yields excellent accuracy for frequencies up to 50 GHz. It can be implemented in the common nonlinear microwave CAD tools and software and was successfully employed with MMIC oscillator design.

Acknowledgment

The authors would like to thank S. Schulz for performing the microwave measurements and M. Rudolph, A. Schüppen, K. Strohm, and J.-F. Luy for valuable discussions.

References

[1] A. Schüppen, U. Erben, A. Gruhle, H. Kibbel, H. Schumacher, and U. König, "Enhanced SiGe heterojunction bipolar transistors with 160 GHz f_{max}," in *Tech. Dig. IEDM 1995*, Dec. 1995, pp. 743–746.

[2] A. Schüppen, A. Gruhle, H. Kibbel, U. Erben, and U. König, "SiGe-HBT's with high f_T at moderate current densities," *Electron. Lett.*, vol. 30, no. 14, pp. 1187–1188, July 1994.

[3] J. E. Gerber, R. Anholt, R. Tayrani, and J. Pence, "A self-heating HBT model for harmonic-balance simulators with parameter extraction," in *1994 Asia Pacific Microwave Conf.*, pp. 1029–1032.

[4] M. E. Hafizi, C. R. Crowell, and M. E. Grupen, "The DC characteristics of GaAs/AlGaAs heterojunction bipolar transistors with application to device modeling," *IEEE Trans. Electron Devices*, vol. 37, pp. 2121–2129, Oct. 1990.

[5] A. Samelis and D. Pavlidis, "A heterojunction bipolar transistor large-signal model for high power microwave applications," in *1995 IEEE MTT-S Dig.*, vol. 3, pp. 1231–1234.

[6] S. Lee and A. Gopinath, "Parameter extraction technique for HBT equivalent circuit using cutoff mode measurement," *IEEE Trans. Microwave Theory Tech.*, vol. 40, pp. 574–577, Mar. 1992.

[7] L. J. Giacoletto, "Measurement of emitter and collector series resistances," *IEEE Trans. Electron Devices*, vol. ED-19, pp. 692–693, May 1972.

[8] C.-J. Wei and J. C. M. Hwang, "Direct extraction of equivalent circuit parameters for heterojunction bipolar transistors," *IEEE Trans. Microwave Theory Tech.*, vol. 43, pp. 2035–2040, Sept. 1995.

[9] M. Rudolph, "Bestimmung des Ersatzschaltbildes von Hetero-Bipolar-Transistoren aus Mikrowellenmessungen," Master's thesis, Technische Universität Berlin, June 1996.

[10] J. E. Getreu, *Modeling the Bipolar Transistor*. Amsterdam, The Netherlands: Elsevier, 1978.

[11] J. F. Luy and P. Russer, *Silicon-Based Millimeter-Wave Devices*. Berlin, Germany: Springer, 1994, Springer Series in Electronics and Photonics.

[12] G. Massobrio and P. Antognetti, *Semiconductor Device Modeling with Spice*, 2nd ed. New York: McGraw-Hill, 1993.

[13] K. Osafune and Y. Yamauchi, "20-GHz 5-DB gain analog multipliers with AlGaAs/GaAs HBT's," in *1991 IEEE MTT-S Dig.*, pp. 1285–1288.

[14] C. Rheinfelder, F. Beisswanger, J. Gerdes, F. Schmückle, K. Strohnm, J.-F. Luy, and W. Heinrich, "A coplanar 38 GHz SiGe-MMIC oscillator," *IEEE Microwave Guided Wave Lett.*, vol. 6, pp. 398–400, Nov. 1996.

Clemens N. Rheinfelder was born in Munich, Germany, in 1965. He received the Dipl.-Ing. degree from the Technical University of Munich in 1993.

Since February 1994, he has been with the Ferdinand-Braun-Institut für Höchstfrequenztechnik Berlin, where he currently is involved in the simulation and design of SiGe monolithic microwave integrated circuits. One of his main tasks is the parameter extraction of small-signal equivalent circuits and the nonlinear modeling of Si–SiGe–Si heterostructure bipolar transistors.

Frank J. Beißwanger was born in Heidenheim, Germany, on December 23, 1968. He received the Dipl. Phys. degree in physics from the University of Ulm, Germany, in 1994, for studies on Si–SiGe heterobipolar structures.

From 1993 to 1996, he was with the Daimler–Benz Research Center in Ulm where his research activities focused on SiGe microwave monolithic integrated circuit (MMIC) technology on high-resistivity silicon substrates and on MMIC design. In 1997, he joined the development department of TEMIC Telefunken Microelectronics, Heilbronn, the semiconductor supplier within the Daimler–Benz group. There he concentrates on RFIC design for communication circuits using TEMIC's SiGe bipolar process.

Wolfgang Heinrich received the Dipl.-Ing., Dr.-Ing., and the Habilitation degrees in 1982, 1987, and 1992, respectively, all from the Technical University of Darmstadt, Germany.

In 1983, he joined the staff of the Institut für Hochfrequenztechnik of Technical University of Darmstadt, where his primary interests included field-theoretical analysis and simulation of planar transmission lines. Since April 1993, he has been with the Ferdinand–Braun-Institut, Berlin, Germany, as head of the microwave department. His present research activities focus on the CAD of microwave monolithic integrated circuit elements and related packaging problems and on microwave circuit design.